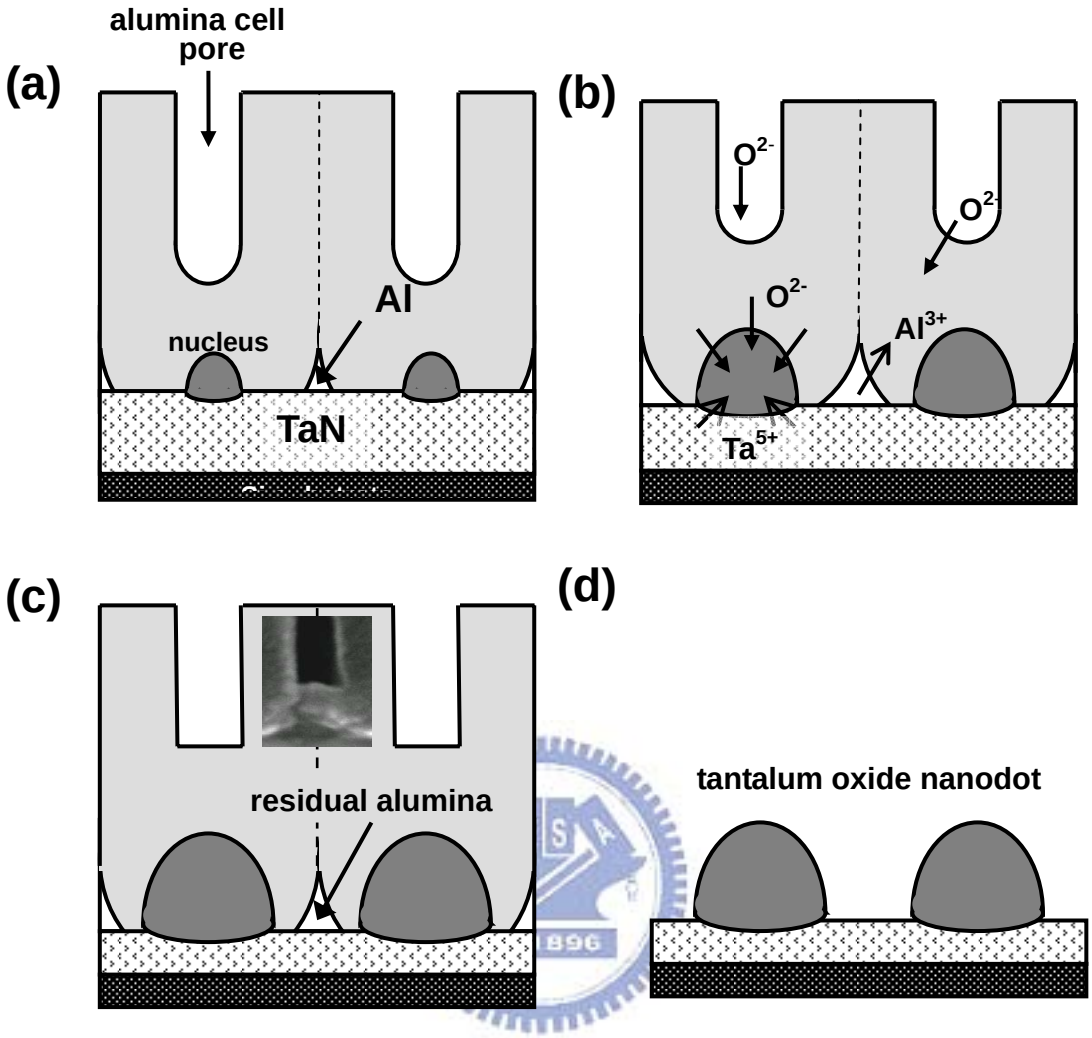

Figure 4-9 Schematic diagrams showing the principal steps of modification of the underlying metal / alumina interface.

At the commencement of current decay, the barrier layer just touches the tantalum surface and the tantala nuclei appear. The residual aluminum is consumed simultaneously with the development of the tantala nanodot until very slight aluminum only remain on the Ta surface around the alumina cells. Thus, the tantala nanodots are separated from each other by alumina and narrow gaps of unoxidised aluminum. The anodization behavior of the barrier layer is very different from the

bulk aluminum case or aluminum on dielectric without Ta. Note that the shape of pore bottom in Figure 4-9 (b) is different forms that in Figure 4-9 (c). While the residual aluminum is consumed, the bases of the alumina pores specifically reshape for the sake of the thickness of the barrier layer in accordance with the constant voltage applied. As a result, the pore bases which are flatten, are shown in Figure 4-9 (c). The volume expansion of tantala nanodots growing, which push the upper alumina forward the pore, may also cause flatted bases of the pores.

4.2.3 Composition Analysis

All samples had been removed overlying alumina layer completely so that the nanodot was directly exposed to the X-ray analysis. The bombardment by ion-gun exhibited fairly smooth morphology and depth profile. Although we didn't know precisely connect the sputter time with the depth of the oxide removed, the profiling data are believed to give us a qualitative assessment of chemical composition throughout the nanodot. Figure 4-10 shows the measured spectrum of the Ta 4f which consists of two doublet peaks ($4f_{7/2}$ and $4f_{5/2}$) have chemical shift relative to the Ta^{5+} state at the handbook of X-Ray Photoelectron Spectroscopy. In the beginning of Ar ion sputtering, the shapes of the Ta 4f doublets do not give any evidence for presence of lower valency oxides in the film composition. It appeared Ta_2O_5 at the surface of nanodot in anodization [16]. The intensity of the tantalum pentoxide doublet decreases with increasing sputtering time. The shift of the Ta 4f peaks toward to lower valency tantalum oxide with sputtering time increased suggests that there may exist different oxidation states of Ta in the depth of the nanodot in despite of the most stable Ta_2O_5 oxide in anodic tantalum oxidation [16]. This implies the transition from stoichiometric Ta_2O_5 at the surface to metallic tantalum with the coexistence of different oxidation states of Ta. One assumption of various tantalum oxides is that the oxidation occurred

too rapidly to form the most stable oxide state. Supposing that unoxidised tantalum does not remain in the hillock composition, it is likely that the presence of metallic tantalum double peak even at the surface of the unsputtered specimen is consistent with metallic tantalum gaps around the hillocks. Figure 4-11 shows different samples which were bombarded by Ar ion sputtering for 6 min. Each of Ta 4f doublet peaks shows the shift toward to lower valency tantalum oxide. However, the support by Surganov et al. [17] indicated that the presence of lower valency tantalum oxides such as TaO, TaO_2 and Ta_2O_3 in the composition of oxide columns formed in similar work. In other words, the top of the nanodot are Ta_2O_5, and the rest of the nanodot is aluminum-free and composed of tantalum pentoxide and comprises other oxidation states of Ta presumably; the degree of tantalum oxidation decreases from the tops of the nanodot towards the interface.

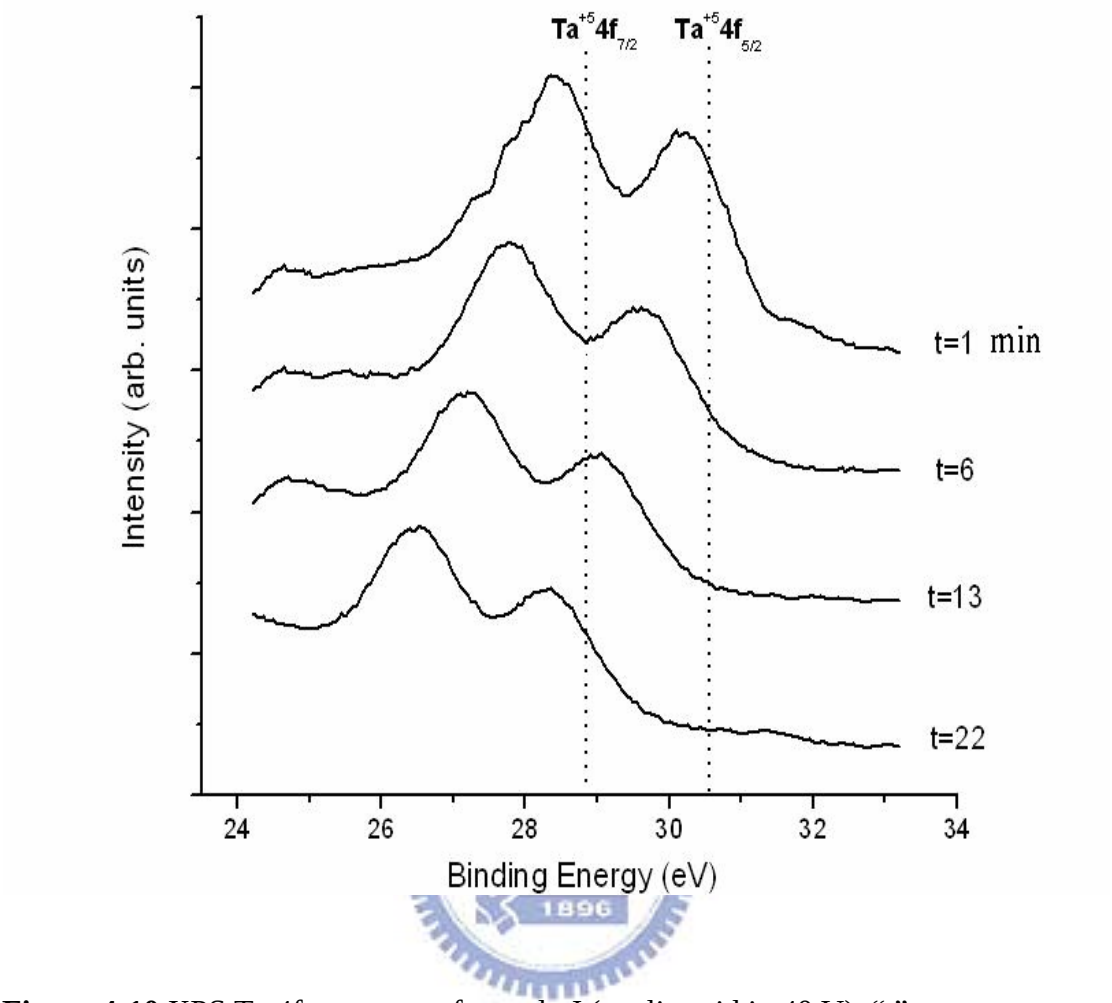

Figure 4-10 XPS Ta 4f spectrum of sample J (oxalic acid in 40 V). "t" means sputtering time.

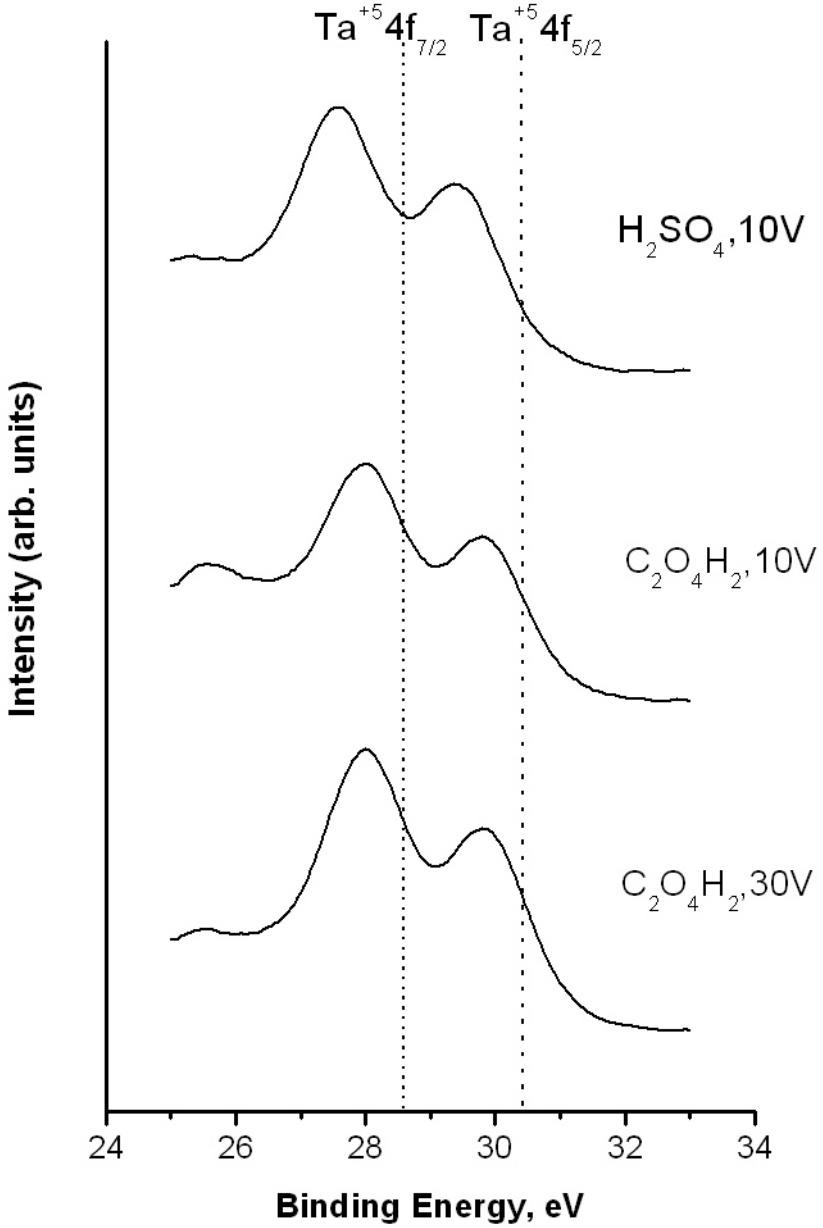

Figure 4-11 XPS Ta 4f spectrum of different sample which sputtered for 3 min.

4.3 Phosphoric acid Specimen

4.3.1 Observations of Nanodot Arrays

Phosphoric acid specimen tantalum oxide nanodot arrays were fabricated in 5wt-% phosphoric acid under 100 constant polarization voltages. Figure 4-12 shows the top-view SEM images of tantalum oxide nanodot arrays. The nanodots of a density 2×10^9 have an average diameter about 200 nm and an average height about 200 nm. Horizontal projections of the bases look like distorted quadrangle rather than hexagons. A distinction of the nanodot differs from the oxalic and sulfuric acid specimen, that is, a spot in the center of the nanodot in Figure 4-12. Contrariously, the shape of the nanodot in phosphoric acid specimen looked like pyramid but hemisphere in oxalic and sulfuric acid specimen. Figure 4-13 indicates the slide-view SEM image of such unusual structure of tantalum oxide nanodot arrays. A thin Pt film coated on nanodots resulted in the rough surface. Figure 4-14 shows slide-view SEM image of tantalum oxide nanodot arrays with unanodized aluminum. The pyramid-like nanodot arrays appeared in phosphoric acid specimen was unexpected but can be duplicated. Figure 4-15 shows the cross-section SEM image of tantalum oxide nanodot arrays with overlying porous alumina film. Unlike oxalic and sulfuric acid specimen, the top of the nanodot was without covered alumina. Figure 4-16 illustrates the cross-section of TEM image of phosphoric acid specimen tantalum oxide nanodot arrays under the alumina film. The pyramid-like nanodots was clearly showed under the bottoms of the alumina pores. The inset SAED (selected area electron diffraction) image shows an amorphous structure of zinc oxide nanodot arrays. The pyramid-like nanodot arrays may be the good field emission material. The geometrical transformation of nanodots between different anodic conditions using porous alumina template caused us to study another mechanism of the nanodot growth.

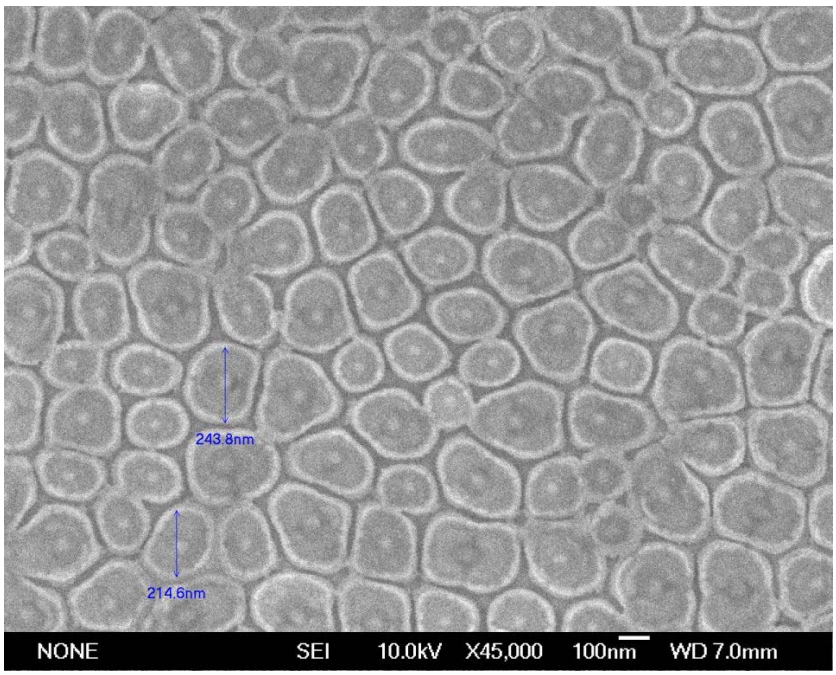

Figure 4-12 Top-view SEM image of tantalum oxide nanodot arrays in 5wt-% phosphoric acid at 100V.

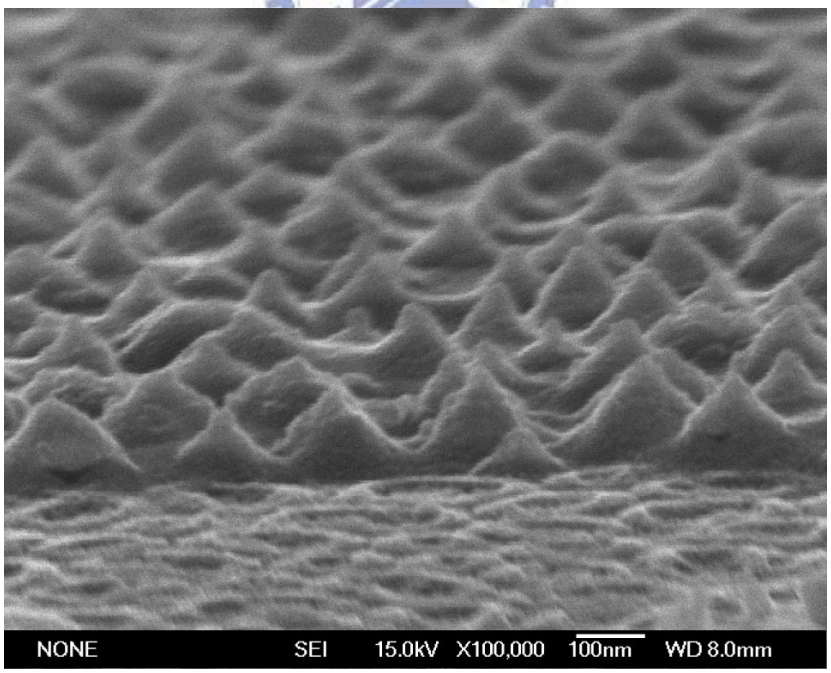

Figure 4-13 Slide-view SEM image of tantalum oxide nanodot arrays in 5wt-% phosphoric acid at 100V.

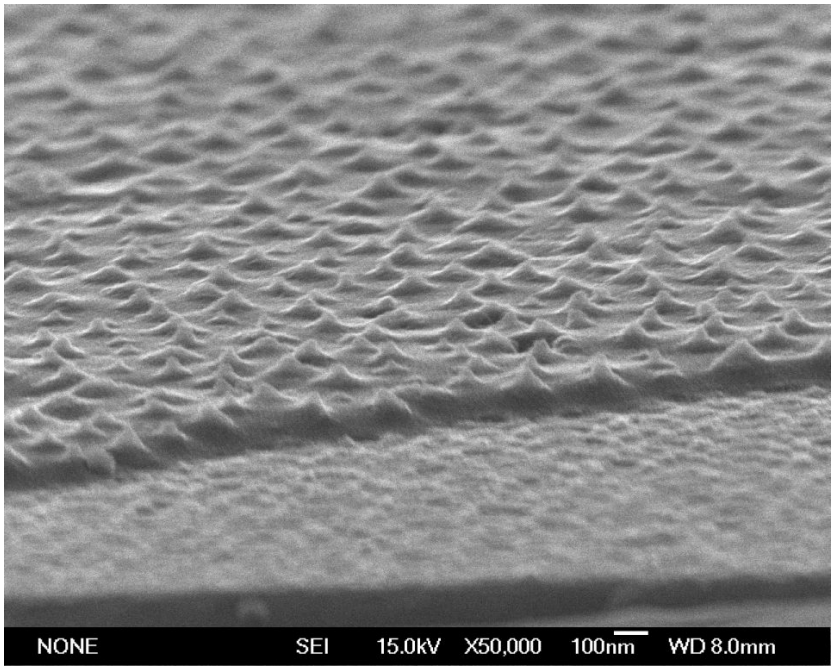

Figure 4-14 Slide-view SEM image of tantalum oxide nanodot arrays with unanodized aluminum.

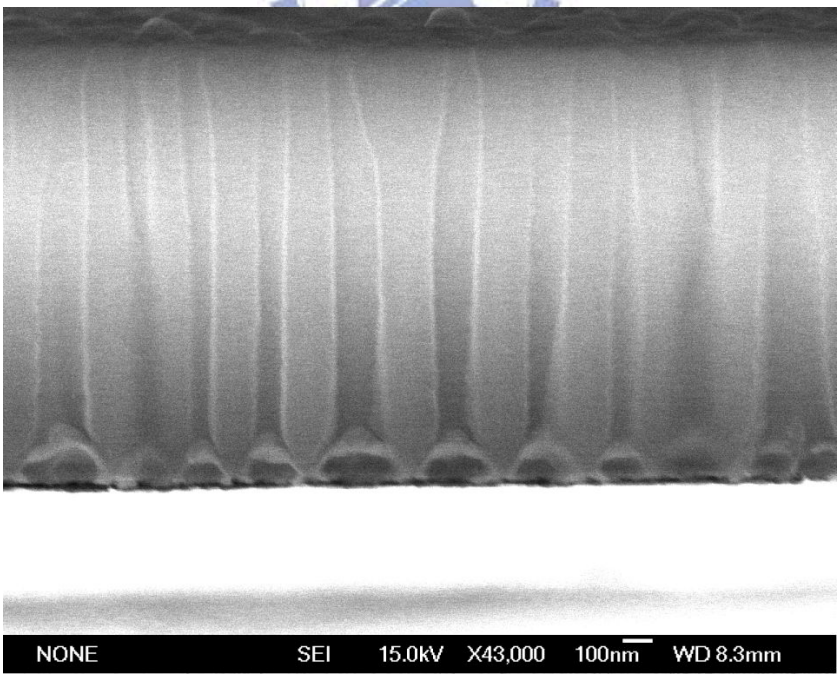

Figure 4-15 Cross-section SEM image of tantalum oxide nanodot arrays with overlying porous alumina film.

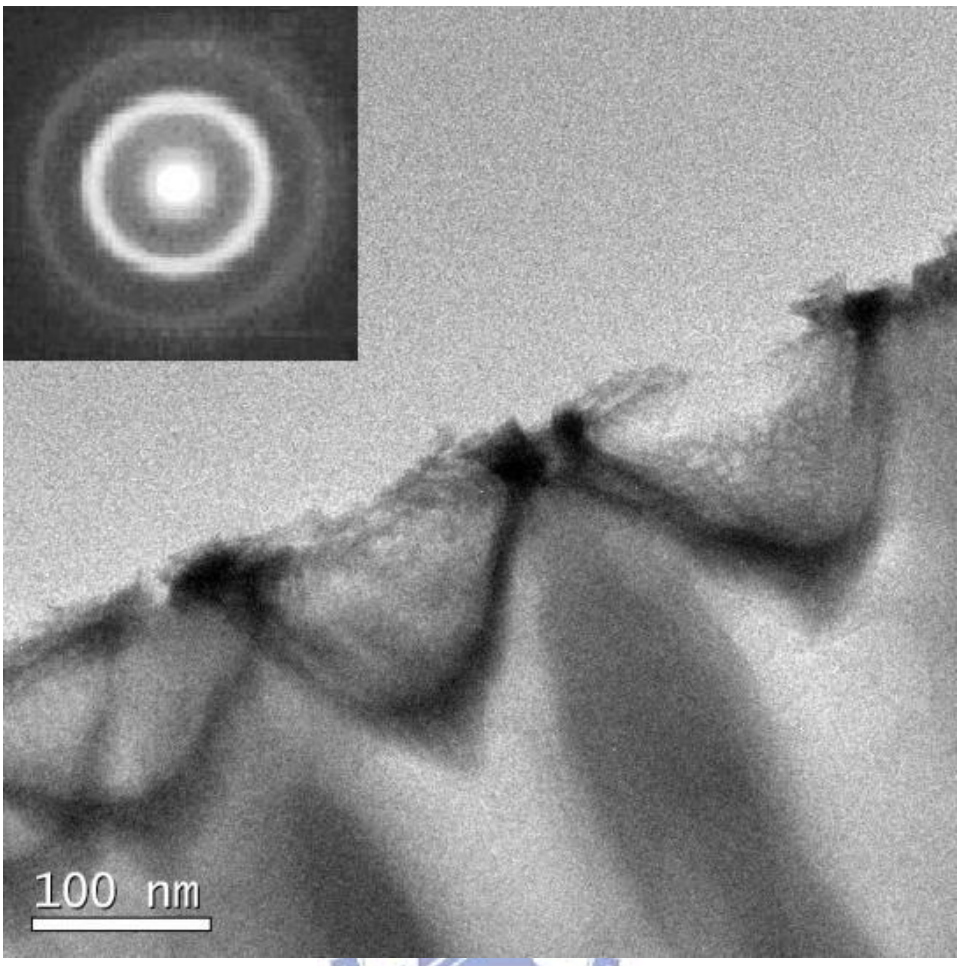

Figure 4-16 TEM image of tantalum oxide nanodot array under the porous alumina film; the inset is the SAED (selected area electron diffraction) image.

4.3.2 Analysis of nanodots

The initial anodization behavior of phosphoric specimen is similar to oxalic and sulfuric specimens. At first, the above aluminum layer oxidized to alumina, accompanied by the outward migration of Al^{3+} and inward diffusion of O^{2-} driven by the applied electric field, leading to the vertical pore channel growth. Furthermore, the bottom of the alumina film consisted of an array of convex hemispheres during the initial anodization, and the position of nanodot had been decided. The alumina dissolution at the alumina /electrolyte interface is in equilibrium with the alumina

growth at the Al/Al_2O_3 interface. As the oxide barrier layer at the pore bottom approaches the Ta/Al interface, the O^{2-} migrating inwards through the alumina barrier layer are continuously injected into the Ta layer and form the tantalum oxide. The O^{2-} released from the dissociated barrier layer at the Ta_2O_5/ Al_2O_3 interface are also injected into the Ta_2O_5 layer, while the released Al^{3+} migrate outwards through the remaining barrier layer and are mostly expelled in the electrolyte. The O^{2-} injected into the Ta_2O_5 layer then migrate inwards and the Ta layer is anodized normally to form new oxide at the Ta/Ta_2O_5 interface. In brief, the underlying tantalum oxide by O^{2-} transported through/from the barrier layer of the initially formed porous alumina without direct contact of Ta with the electrolyte. The tantalum oxide nanodot resulting from oxidation of the Ta layer is accompanied by a volume expansion. The continued consumption of the adjacent aluminum enhances expansion of nanodots in horizontal direction and, simultaneously, is accompanied by further dissolution of the barrier layer until phosphoric acid directly contact the top of nanodots without barrier alumina layer as showed in Figure 4-15. The growing nanodots punched through alumina barrier didn't appear in oxalic and sulfuric specimens. There are two reasons to verify：First, the high local electric field caused the violent expansion of nanodot. Second, the etching rate of phosphoric acid to alumina in such anodizing condition is far faster than oxalic and sulfuric acid. It may be due to the remainder of alumina barrier layer, which did not dissolve completely and was pushed outwards from its initial position by growing tantalum oxide during the current decay period. Once this happens, the electrolyte may directly penetrate between the top of nanodot and corresponding alumina cells, allowing further direct oxidation and evolution of nanodots to their final shape, shown in Figure 4-17 (C). The direct contact of tantalum with the electrolyte caused the further oxidation of tantalum. Although the top of nanodots can reach the electrolyte, the residual alumina of sideward pores blocked the

growth of the base part of nanodots. As a result, a pyramid-like nanodot arrays were appeared.

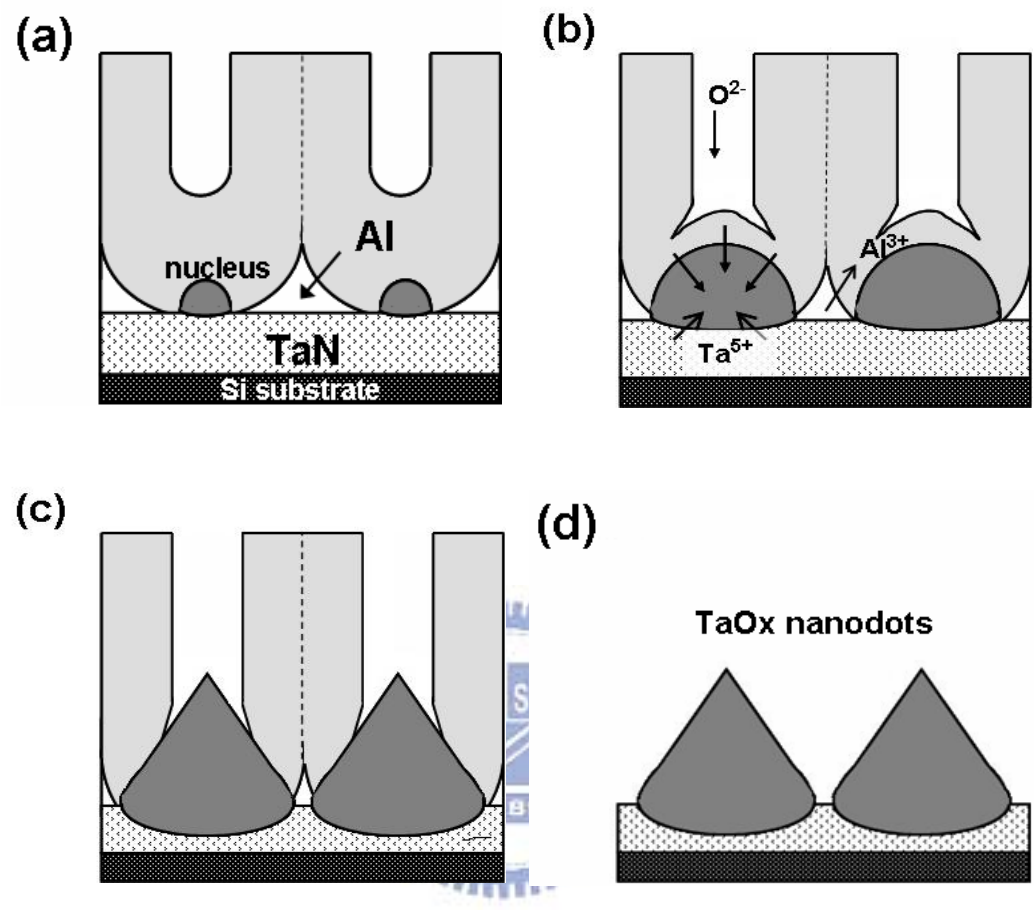

Figure 4-17 Schematic diagrams showing the principal steps of modification of the underlying metal / alumina interface in phosphoric acid specimen.